Cosmic Spectroscopy (a Test for "Nearby" UHECR Sources)

Tom Weiler
Vanderbilt University
Nashville, TN
co-authors: L. Anchordoqui, V. Barger

Prob(E,Z,A,xB,D), with multi-correlated parameters, built upon four simple observations:

1. from GZK, higher E, <=> fewer local sources
2. from GZK/photonuclear prod'n,
    1. higher E <=> higher A
3. higher E <=> smaller angular bending
4. local discreteness must be considered (cosmic variance, ensemble averaging)

Luis' figure says a lot:

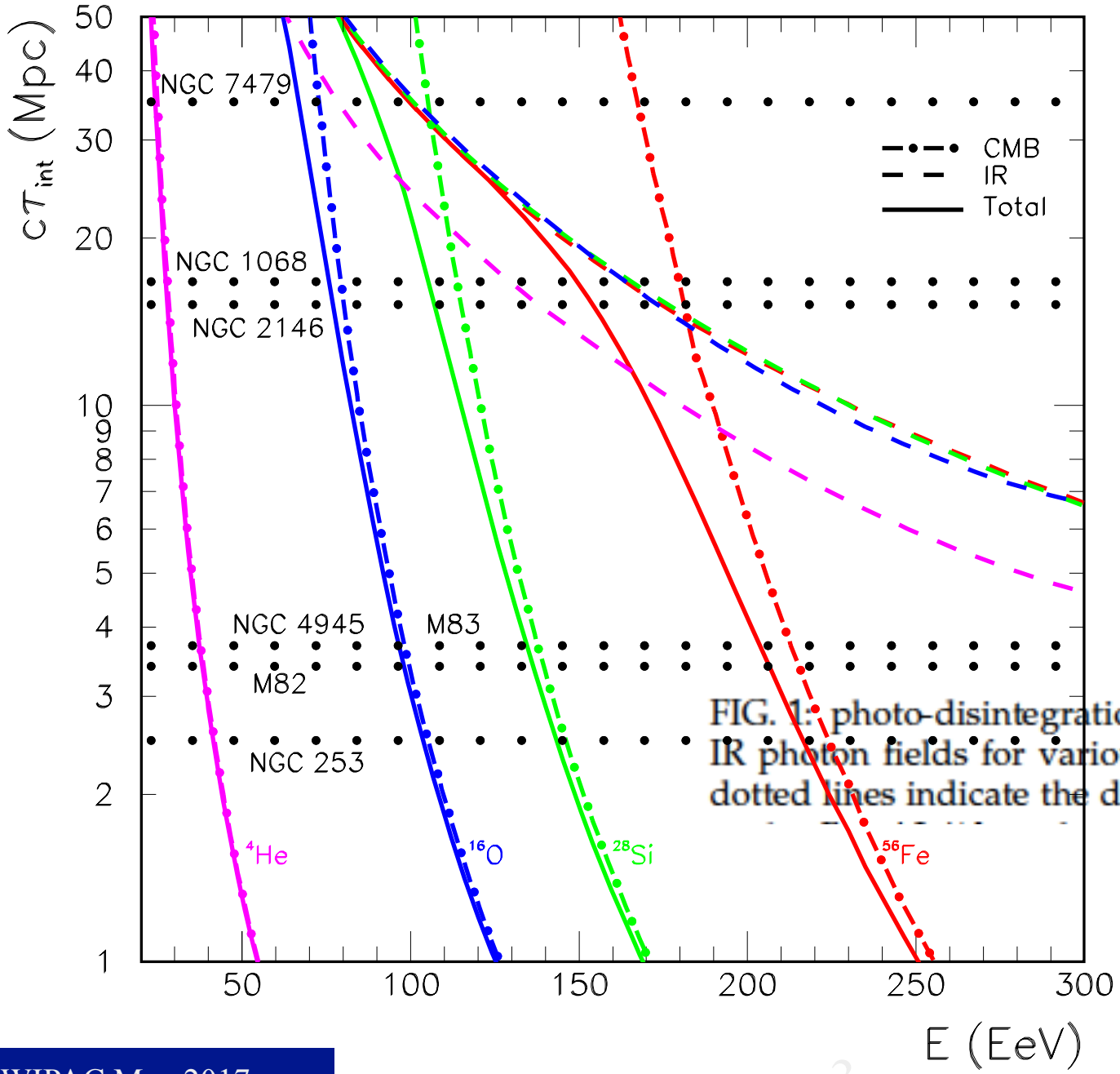

FIG. 1: photo-disintegration mean free path on the CMB and IR photon fields for various nuclear species. The horizontal dotted lines indicate the distance to nearby starburst galaxies

ie,

interaction mean free path (mfp) decreases rapidly with increasing energy, and increases rapidly with increasing nuclear composition:

- at $E = 10^{10.6}$ GeV, the mfp for ionized helium (^{4}He) is about 3 Mpc, while at $10^{10.85}$ GeV it is nil;
- at $E = 10^{11}$ GeV, the mfp for ionized oxygen (^{16}O) is about 4 Mpc, while at $10^{11.2}$ GeV it is nil;
- It $E = 10^{11.2}$ GeV, the mfp for ionized silicon (^{28}Si) is about 2.5 Mpc, while at $10^{11.3}$ GeV it is nil;
- etcetera, until finally we reach ionized iron (^{56}Fe) where the mfp at $E = 10^{11.3}$ GeV is about 4 Mpc, while at $10^{10.44}$ GeV it too is nil.

predicts that:

- the contribution of ^{4}He should decrease with rising energy and then essentially disappear above about $10^{10.7}$ GeV;
- on average, only species heavier than ^{16}O can contribute to the observed flux on Earth above 10^{11} GeV, with nuclear species lighter than ^{28}Si highly suppressed at $10^{11.6}$ GeV;
- the mean flux of iron nuclei becomes suppressed somewhat below $10^{11.4}$ GeV. This is the maximum average energy expected on Earth, and is in agreement at the 1σ level with Fly's Eye observations [26].

An apparent correlation between UHECRs and nearby starbursts is visible in Fig. 4. As a matter of fact, the Pierre Auger Collaboration has recently reported an indication of a possible correlation between UHECRs ($E > 3.9 \times 10^{10}$ GeV) and starburst galaxies, with an *a posteriori* chance probability in an isotropic CR sky of $p_{\rm Auger} = 4.2 \times 10^{-5}$, corresponding to a 1-sided Gaussian significance of 3.9σ [64, 65].[3] In addition, the possible association of the TA hot spot with M82 has not gone unnoticed [66–68]. The combined p-value for the two non-correlated observations is

$$p = p_{\rm TA} \otimes p_{\rm Auger} = 1.5 \times 10^{-8}, \qquad (12)$$

yielding a statistical significance $\gtrsim 5\sigma$. However, caution must be exercised in all-sky comparisons [69]. Moreover, in (12) we have combined a catalog-based search (Auger) with a blind search (TA). Therefore, (12) provides a rough estimate of the statistical significance under the strong assumption that M82 (which is at the border of the excess of events) is the only source contributing to the TA hot spot. It is clear that new data are needed to confirm

Starburst Galaxies:

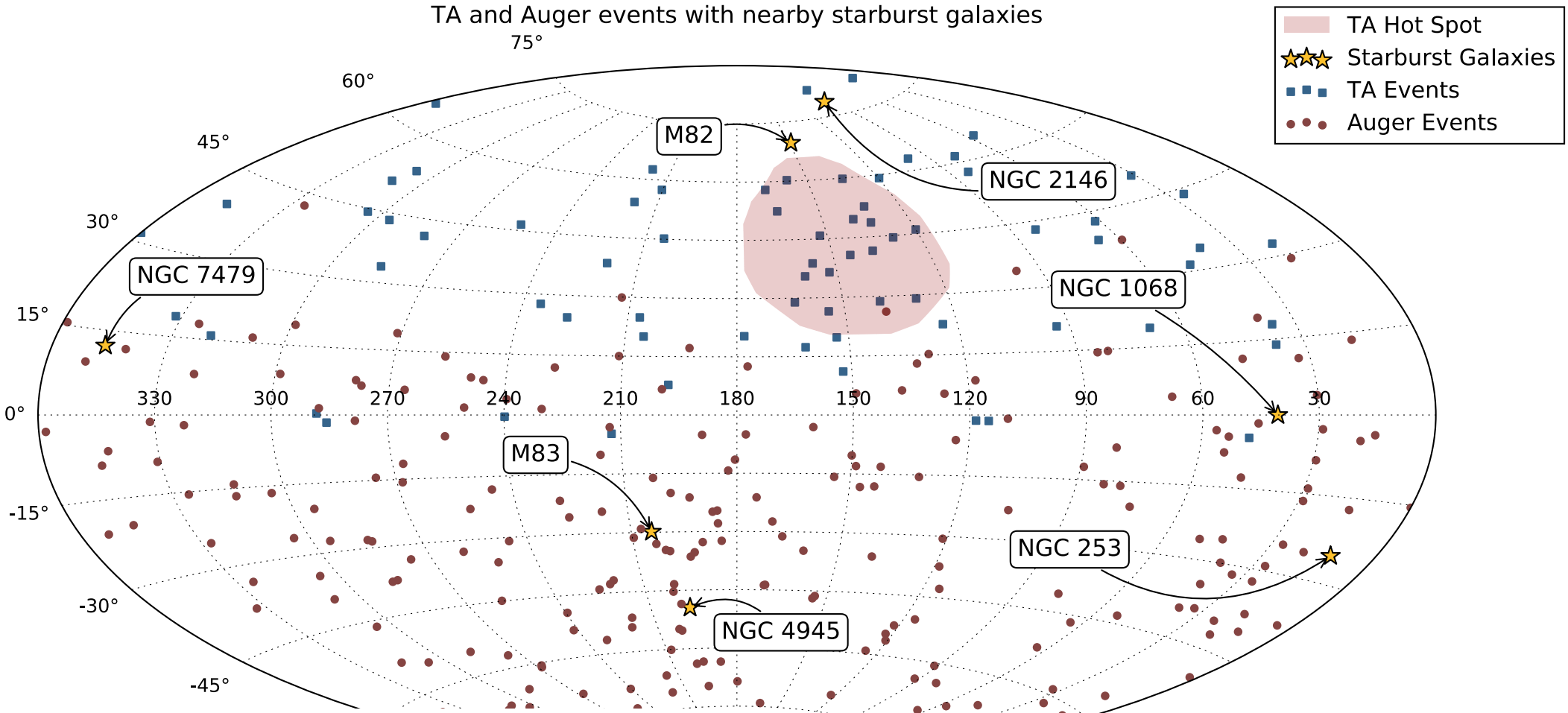

FIG. 4: Comparison of UHECR event locations with nearby starburst galaxies in equatorial coordinates, with R.A. increasing from right to left. The circles indicate the arrival directions of 231 events with $E > 52$ EeV and zenith angle $\theta < 80°$ detected by the Pierre Auger Observatory from 2004 January 1 up to 2014 March 31 [63]. The squares indicate the arrival directions of 72 events with $E > 57$ EeV and $\theta < 55°$ recorded from 2008 May 11 to 2013 May 4 with TA [17]. The stars indicate the location of nearby (distance < 50 Mpc) starburst galaxies. The shaded region delimits the TA hot-spot.

Starburst Postulate is Testable:

four likely starburst candidates within 4 Mpc of Earth, and two more at ~ 15 Mpc from Earth. We get:

- the maximum average energy of nuclei arriving from the direction of NGC 2146 and/or NGC 1068 is roughly $10^{11.2}$ GeV;
- no ions lighter than ^{28}Si would be observed from NGC 2146 and/or NGC 1068 with an average energy beyond $10^{11.13}$ GeV.

Earlier, prescient, influential papers:

Loeb and Waxman (astro-ph/0601695)

He, Kusenko, … (1411.5273)

…, Kamionkowski, …(1512.04959)

eg, H.-N. He, A. Kusenko, …

Source Name	Source Type	Distance (Mpc)	RA (°)	Dec (°)	α (°)	A_1 (°)	A_2 (°)	$P/P_{\text{best-fit}}$ (%)
best-fit	-	-	$142.8^{+47.8}_{-49.0}$	$69.2^{+11.7}_{-27.6}$	$185.7^{+106.8}_{-121.2}$	$17.4^{+17.0}_{11.0}$	$9.4^{+2.7}_{-0.3}$	100
M82	starburst galaxy	3.4	149.0	69.7	174.2	17.6	9.6	99.8
UCC 05101	star-forming galaxy	160.2	143.0	61.5	182.9	11.6	9.2	96.9
Mrk 180	blazar	185	174.1	70.2	136.1	19.9	9.3	91.3
UCC 03967	galaxy cluster	150.3	115.2	55.4	253.4	14.9	9.5	67.4
A 0576	galaxy cluster	169.0	110.4	55.7	259.0	17.0	9.4	63.4
Arp 55	star-forming Galaxy	162.7	138.2	44.5	279.6	1.9	9.7	55.3
Arp 148	star-forming Galaxy	143.3	165.3	41.1	69.3	10.5	10.0	41.8
Mrk 421	blazar	134	166.1	38.2	61.5	11.2	9.9	35.6

Starburst Galaxies:

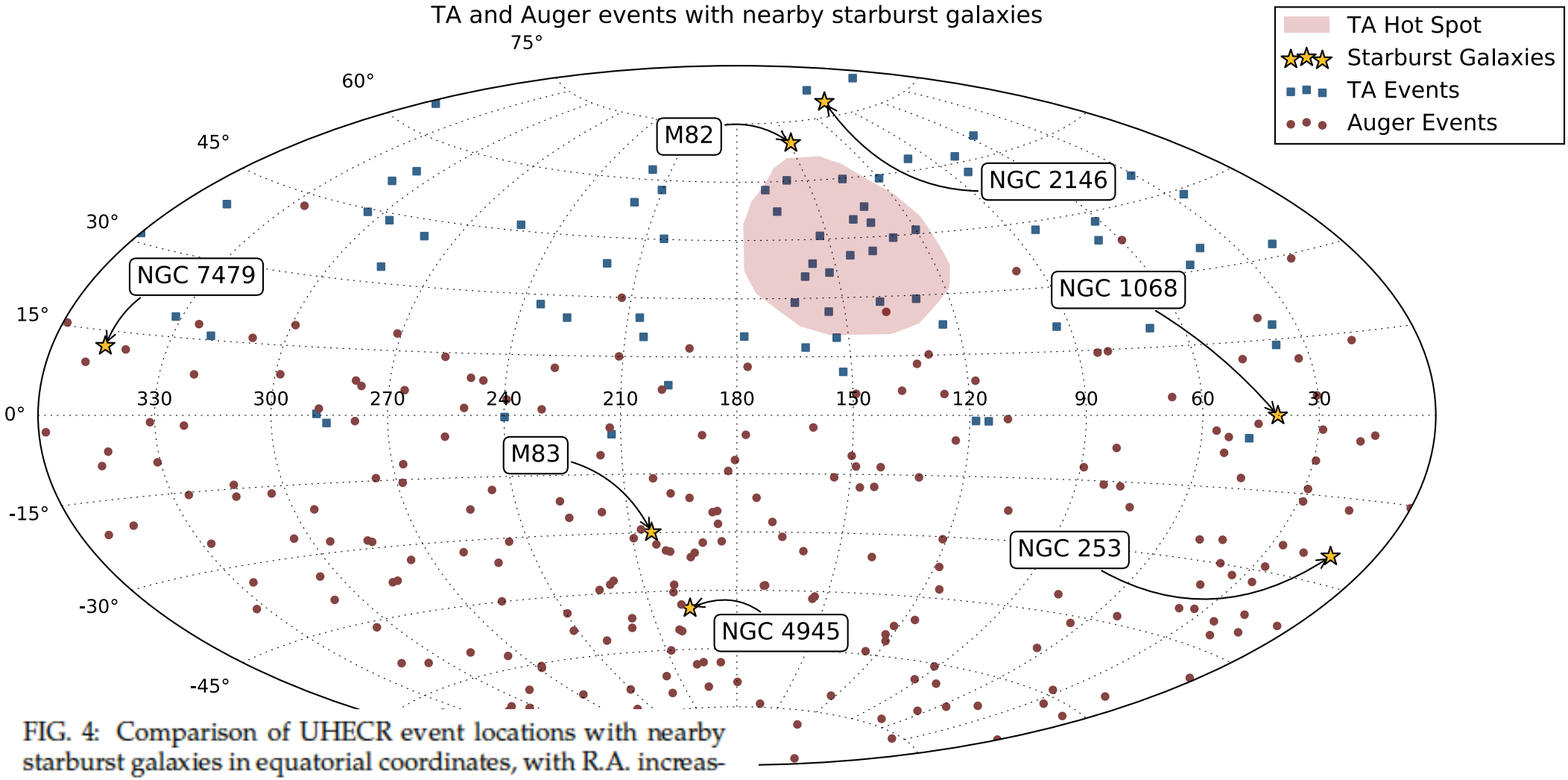

FIG. 4: Comparison of UHECR event locations with nearby starburst galaxies in equatorial coordinates, with R.A. increasing from right to left. The circles indicate the arrival directions of 231 events with $E > 52$ EeV and zenith angle $\theta < 80°$ detected by the Pierre Auger Observatory from 2004 January 1 up to 2014 March 31 [63]. The squares indicate the arrival directions of 72 events with $E > 57$ EeV and $\theta < 55°$ recorded from 2008 May 11 to 2013 May 4 with TA [17]. The stars indicate the location of nearby (distance < 50 Mpc) starburst galaxies. The shaded region delimits the TA hot-spot.

Starburst Galaxies

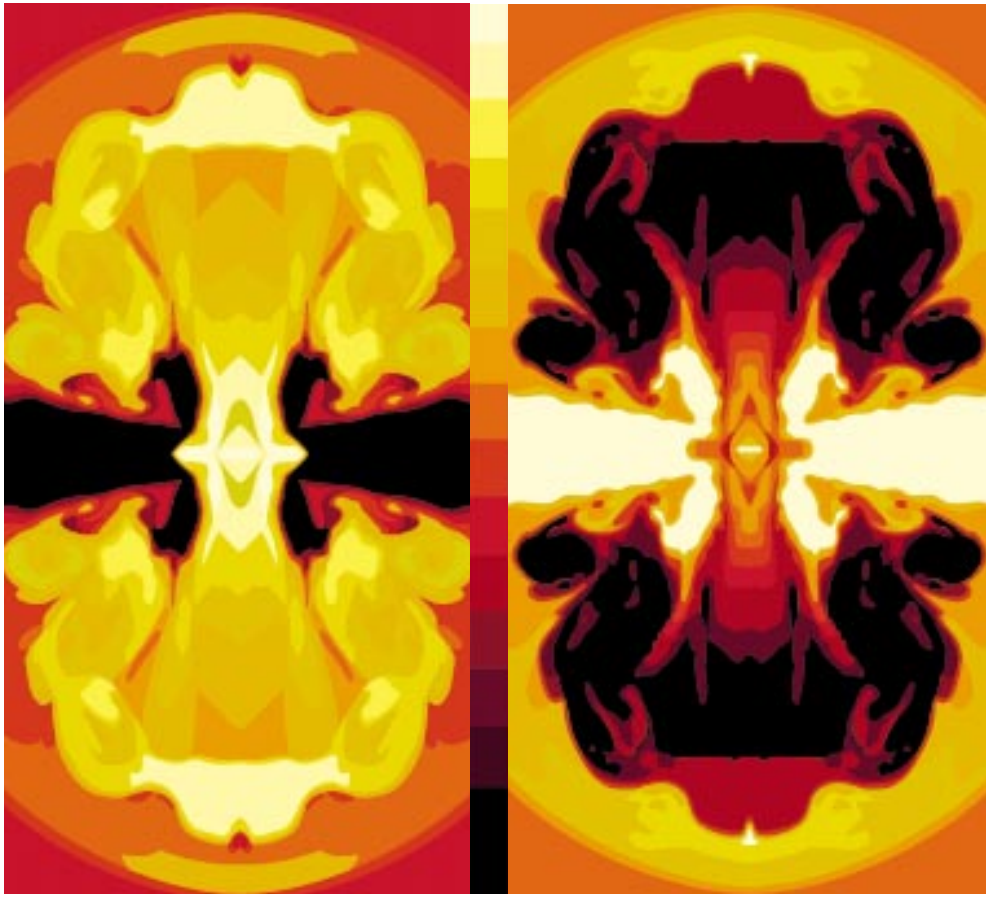

FIG. 2: Numerical simulation of a starburst's superwind. *Left panel*. Temperature map (bright = hot) showing how the hot gas emanating from the nucleus displaces the cooler galactic gas around it. *Right panel*. Gas density map (bright = dense) showing the inhomogeneous outflow along the rotation axis of the disk composed of a series of hot, dense, and fast shock fronts of material that are trailed by gas which has expanded, cooled, and slowed down. This figure is courtesy of Gerald Cecil [39].

FIG. 3: Telescopic snapshot of M82. Shortly after the identification of optical emission-line filaments [40] it became widely accepted that M82 is the archetype starburst galaxy [41]. The huge lanes of dust that crisscross the disk of M82 are the telltale signature of the flurry of star formation. Winds from massive stars and blasts from supernova explosions have created a strong superwind of galactic-scale, which is spewing knotty filaments of hydrogen and nitrogen gas [42, 43]. The red-glowing outwardly expanding filaments featuring the Hα emission provide direct evidence for the galactic-scale superwind emanating from the central region to the outer halo area. This figure is courtesy of Leonardo Orazi.

At issue, pointed out by Ahlers et al, contribution of Starburst Galaxies to IceCube nu flux is naively too LOW !

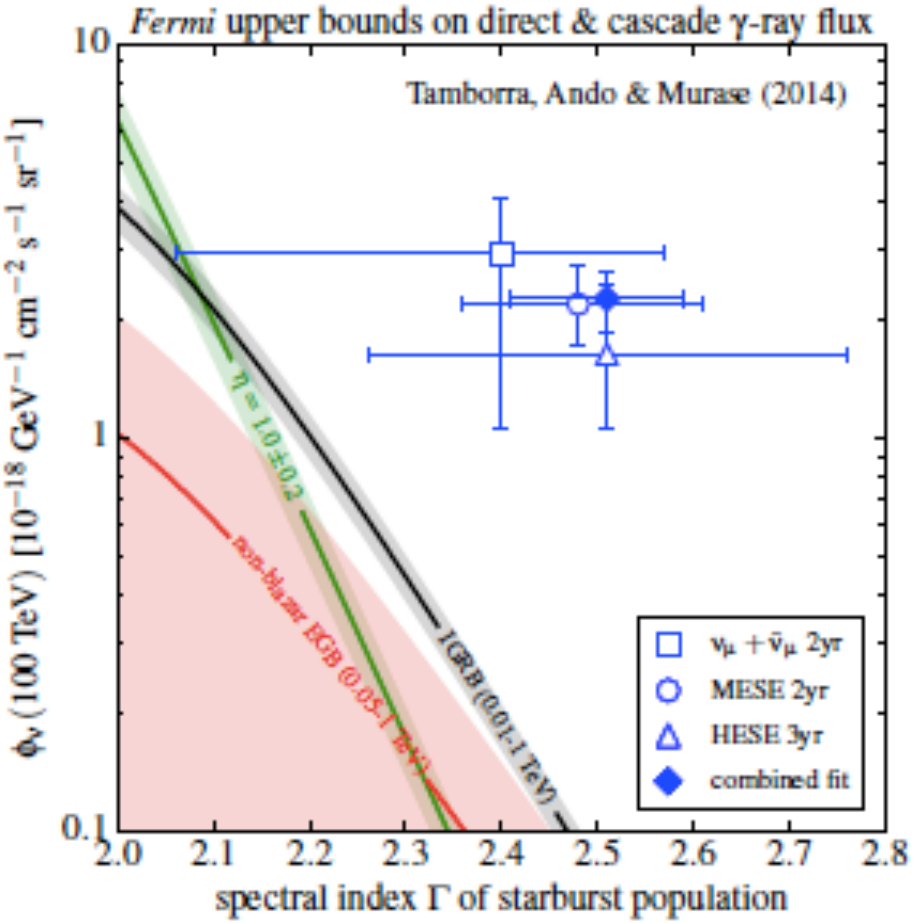

Figure 3. Upper limits on the per-flavor normalization $\phi_\nu(100\mathrm{TeV})$ of SFGs depending on the starburst spectral index Γ_{SB}. The model of Tamborra et al. (2014) is restricted to the green band where we allow for a 20% uncertainty of the absolute normalization from the IR-γ-ray correlation. The black and red lines show the upper limits from the IGRB (0.01–1 TeV) and from the non-blazar EGB (0.05–1 TeV), respectively. Both results are shown with uncertainty bands. The data points show the best-fit power-law neutrino spectrum including the 68% C.L. range in terms of the spectral index Γ and astrophysical normalization at 100 TeV estimated by IceCube analysis: the high-energy starting event (HESE) analysis (Aartsen et al. 2014b), the medium-energy starting event (MESE) analysis (Aartsen et al. 2015b) and the classical search for up-going $\nu_\mu + \bar{\nu}_\mu$ tracks (Aartsen et al. 2015c). The values are extracted from Aartsen et al. (2015a), which also derives a combined fit to the data.

But see Murase/Waxman (1607.01608) for E^{-2}, … K. Fang for choked sources, or postulate separate, designer (DM?) source

Conclusions:

"ensemble fluctuations" important,
may well determine source(s) of UHECRs.
We feel Starbursts are a contributor.
("Competition" exists: - the Blazer crowd
Kamionkowski et al, Tidal Disruptions (1512.04959)
Hooper et al - Radio Galaxies (1612.06462)
- etc.

μ

A few might be correct !

Extra Slides

from Ahlers et al:

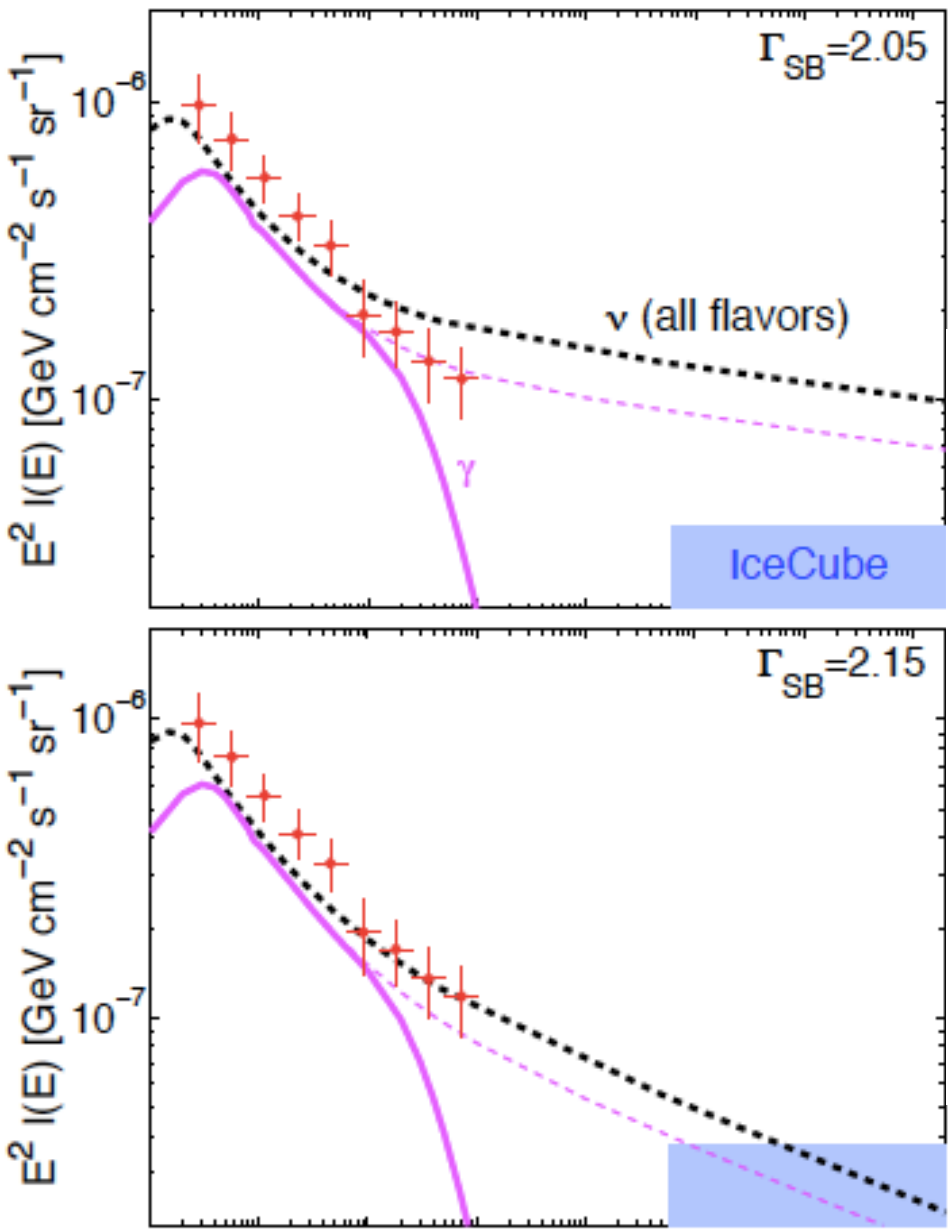

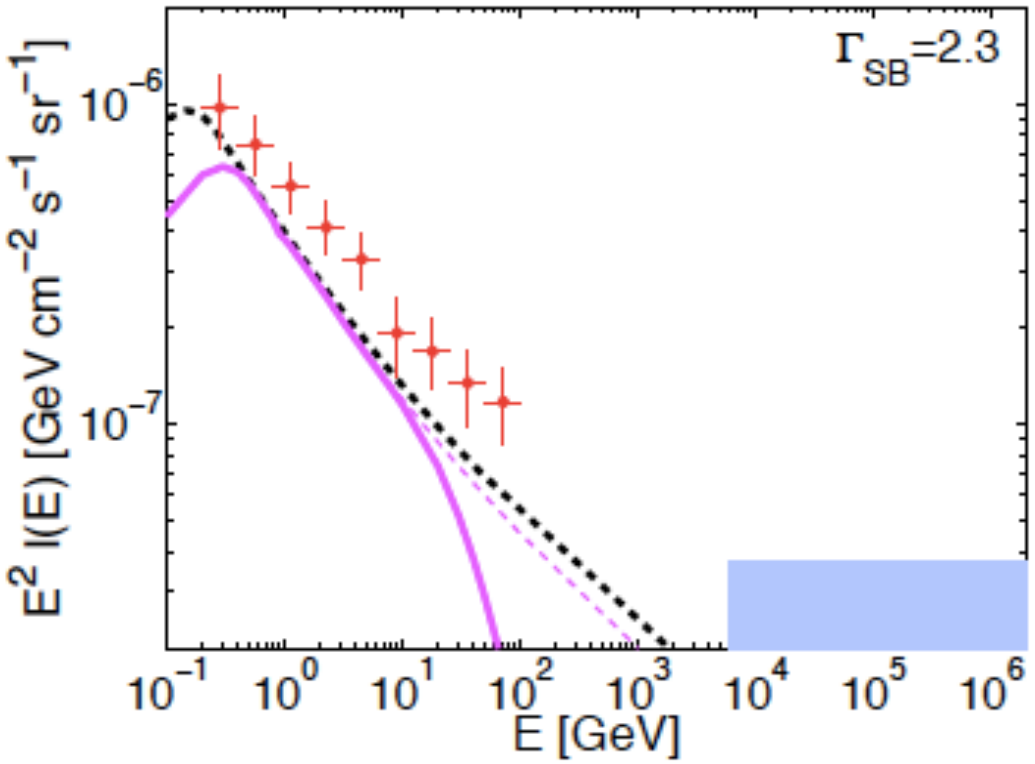

Figure 5. Diffuse gamma-ray (in magenta) and neutrino intensity (in dashed black) $E^2I(E)$ as a function of the energy for our canonical model, assuming $\Gamma_{SB} = 2.05, 2.15$ and 2.3 (from top to bottom). The *Fermi* data [5] are marked in red, while the IceCube region is plotted in light blue [35].

Glashow's peak:

$$\sigma_{\mathrm{Res}}^{\mathrm{peak}} = \frac{24\pi\,\mathrm{B}(W^- \to \bar{\nu}_e e^-)\,\mathrm{B}(W^- \to \mathrm{had})}{M_W^2}$$
$$= 3.4 \times 10^{-31}\,\mathrm{cm}^2\,.$$

J.G.Learned and T.J. Weiler, arXiv:1407.0739

Neutrino Energy Maximum:

$$E_\nu^{\max} = \frac{m_\nu \, M_{\rm Planck}}{M_{\rm weak}}$$

$$= 2.5 \left(\frac{m_\nu}{0.05\,{\rm eV}}\right) \left(\frac{M_{\rm Planck}}{1.2\times 10^{28}\,{\rm eV}}\right) \left(\frac{247\,{\rm GeV}}{v_{\rm weak}}\right) {\rm PeV}\,.$$

In what frame?

Nature provides THE preferred frame, the Cosmic Rest Frame.
So $E_\nu^{\max}$ can be written as $u_\beta^{\rm CRF}(p_\nu^{\max})^\beta\,, \quad$ where $u_\beta^{\rm CRF} = (1,\vec{0})$.

And $(p_\nu^{\max})^\beta$ transforms as usual four-vector.

Neutrino maximum energy (cont.) another way:

Weingberg's neutrino-mass generating operator,

$$\frac{1}{\Lambda}(HL)(HL) => m_\nu = \frac{vev^2}{\Lambda},$$

$m_\nu \sim \frac{\mathrm{vev}^2}{\mathrm{M_{GUT}}}$, so

$$\Gamma_\nu(E_\nu \sim \mathrm{PeV}) = \frac{E_\nu}{m_\nu} \sim \left(\frac{\mathrm{PeV}}{\mathrm{vev}}\right)\left(\frac{M_{\mathrm{GUT}}}{M_P}\right)\left(\frac{M_P}{\mathrm{vev}}\right),$$

$$\sim 10^4 \times 10^{-4} \times \left(\frac{M_P}{\mathrm{vev}}\right).$$

The End of the Neutrino Spectrum

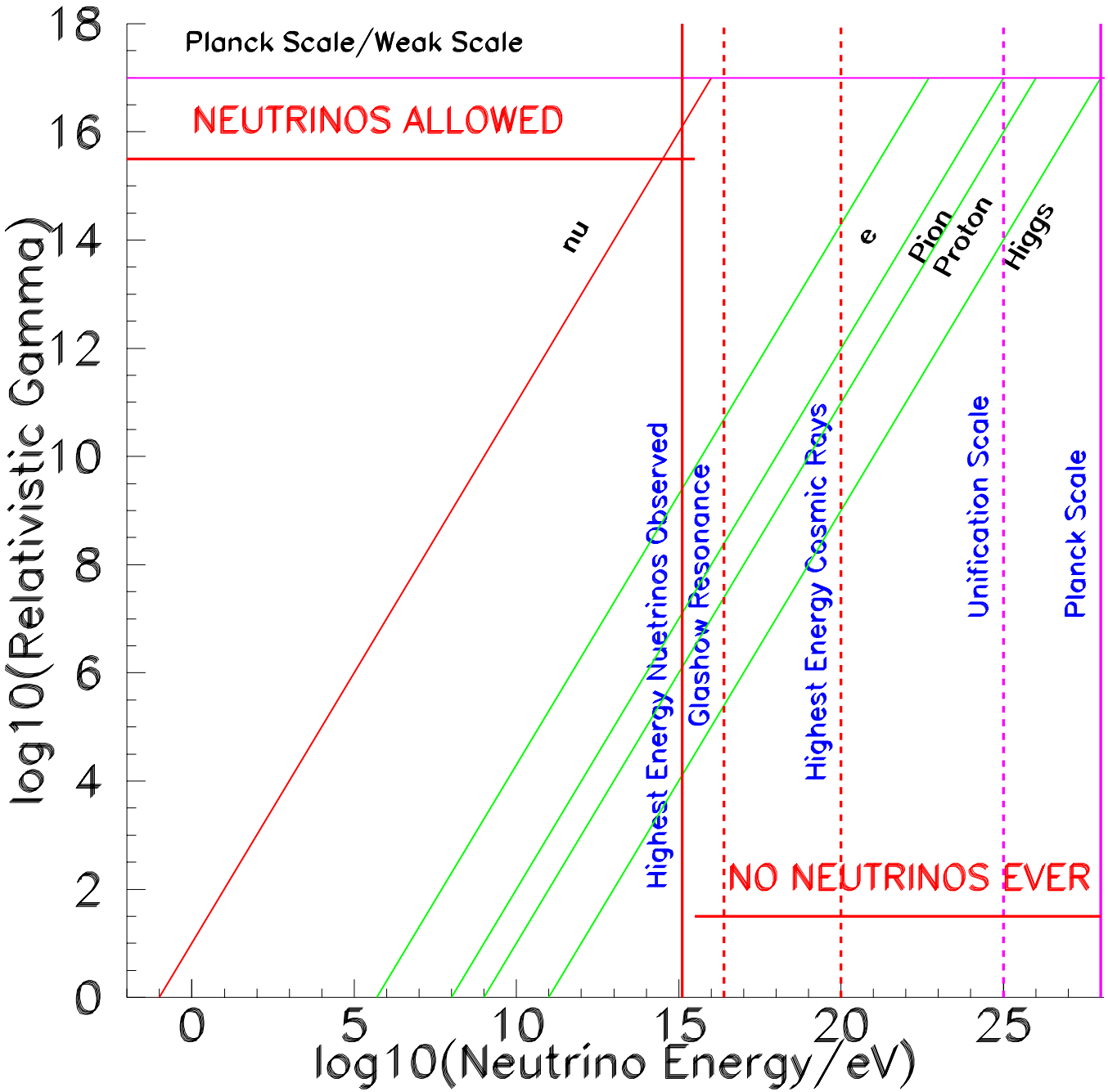

Learned & TJW (2014)

Glashows may receive help from IceCube Gen-2:

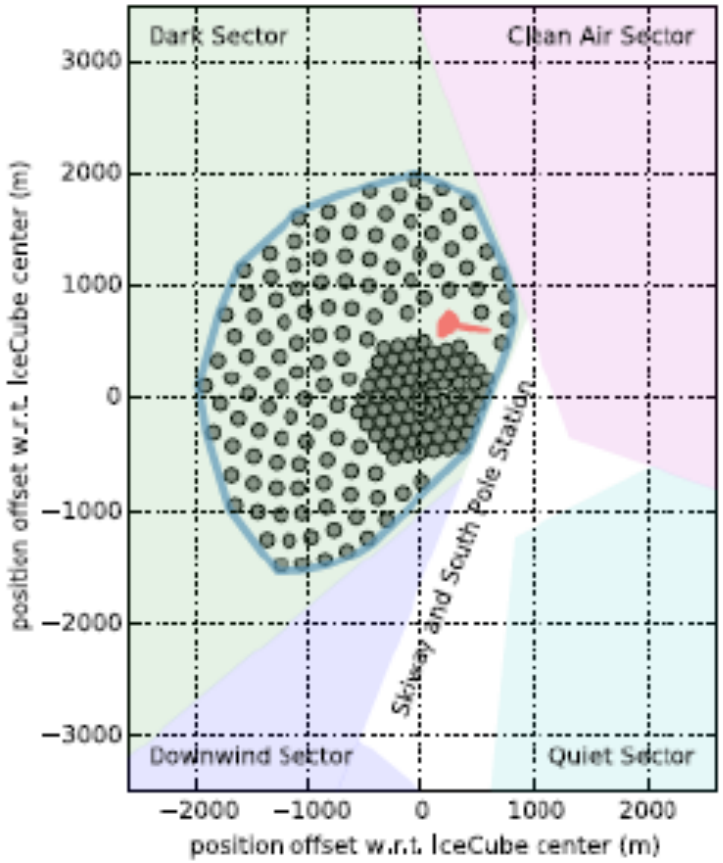

STRAWMAN DETECTOR

- 120 additional strings
- length 1.3 km
- average spacing 240 m
- volume 9.7 km^3

Glashow Resonance - Formulas:

$$\left(\frac{N}{T\Omega}\right)_{\rm Res} = \frac{N_p}{2m_e}\left(\pi M_W \Gamma_W\right)\sigma_{\rm Res}^{\rm peak}\left.\frac{dF_{\bar{\nu}_e}}{dE_{\bar{\nu}_e}}\right|_{E_{\bar{\nu}_e}=6.3{\rm PeV}},$$

$$\sigma_{\rm Res}^{\rm peak} = \frac{24\pi\,{\rm B}(W^- \to \bar{\nu}_e e^-)\,{\rm B}(W^- \to {\rm had})}{M_W^2} = 3.4\times 10^{-31}{\rm cm}^2\,.$$

Glashow event rates vs. continuum:

TABLE II: Ratio of resonant event rate around the 6.3 PeV peak to non-resonant event rate above $E_\nu^{\rm min} = 1,\ 2,\ 3,\ 4,\ 5$ PeV. The single power-law spectral index α is taken to be 2.0 and 2.3 for the non-parenthetic and parenthetic values, respectively. As an example, the single power-law extrapolation from the three events observed just above 1 PeV predicts a mean number of observed resonance events around 6.3 PeV equal to the first numerical column times 3.

$E_\nu^{\rm min}$ (PeV)	1	2	3	4	5
$pp \to \pi^\pm$ pairs	0.33 (0.29)	0.50 (0.53)	0.64 (0.77)	0.76 (1.0)	0.87 (1.2)
damped $\mu^\pm$	0.22 (0.18)	0.33 (0.34)	0.42 (0.50)	0.49 (0.64)	0.56 (0.79)
$p\gamma \to \pi^+$ only	0.14 (0.12)	0.22 (0.23)	0.28 (0.33)	0.33 (0.43)	0.38 (0.53)
damped μ^+	0 (0)	0 (0)	0 (0)	0 (0)	0 (0)
charm decay	0.37 (0.32)	0.56 (0.60)	0.72 (0.86)	0.85 (1.1)	0.98 (1.4)
neutron decay	1.1 (0.94)	1.7 (1.8)	2.1 (2.5)	2.5 (3.3)	2.9 (4.0)